

Supplementary Material for

Rational design of a small organic photosensitizer for NIR-I imaging-guided synergistic photodynamic and photothermal therapy

Shibo Lv,^{#a} Yuhan Liu,^{#a} Yanliang Zhao,^a Xiaoxue Fan,^a Fangyuan Lv,^a
Erting Feng,^b Dapeng Liu,^{* a} Fengling Song^{* a,b}

a. Institute of Molecular Science and Engineering, Institute of Frontier and
Interdisciplinary Science. Shandong University, Qingdao, Shandong, 266237,
China

b. State Key Laboratory of Fine Chemicals, Dalian University of Technology, No.
2 Linggong Road, High-tech District, Dalian, China

Materials and methods

4,8-dibromo-6-(2-ethylhexyl)-[1,2,5] thiadiazole [3,4-F] benzotriazole (Br-BTZ) was purchased from Zhiyan company, Nanjing, China. N-(Carbonyl-methoxypolyethylene glycol-2000)-1,2-distearoyl-sn-glycero-3-phosphoethanolamine (PEG2000), Tetrakis(triphenylphosphine)palladium, 1,3-diphenylisobenzofuran (DPBF), 4-(Diphenylamino)phenylboronic acid, 4',6-diamidino-2-phenylindole (DAPI), and 3-(4,5-dimethylthiazol-2-yl)-2,5-diphenyltetrazolium bromide (MTT) was obtained from Energy Chemical, Shanghai, China. Singlet oxygen sensor Green (SOSG), hydroxyphenyl fluorescein (HPF), dihydrorhodamine 123 (DHR123), dihydroethidium (DHE), and 2',7'-dichlorofluorescein diacetate (DCFH-DA) was obtained from life technologies corporation. Minimum essential medium (MEM), RPMI 1640 Medium and penicillin-streptomycin were purchased from Genview Company, and Fetal Bovine Serum (FBS) was obtained from Scitecher Company.

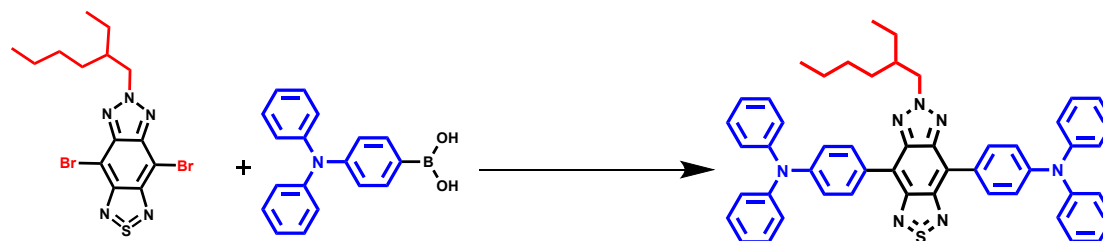
Multinuclear NMR spectra including ¹H NMR and ¹³C NMR spectra were obtained on a Bruker Ascend-600 spectrometer. ESI-TOF-MS measurements were conducted on a high resolution LTQ-Orbitrap mass spectrometer with ETD. UV-Vis measurements

were performed on the HITACH UH5300 and fluorescence spectra (FL) were taken on FLS1000 Photoluminescence Spectrometer from Edinburgh Instruments. The fluorescence lifetimes were obtained by time-correlated single photon counting (TCSPC) method. And the absolute fluorescence quantum yields were calculated based on the integrating sphere mode on The FLS1000 from Edinburgh Instruments. The optical length in the reported UV-Vis, FL, luminescence lifetime, and NTAS measurements was 1 cm unless otherwise mentioned. Electron spin resonance (ESR) measurements were carried out on a Bruker Model A300 spectrometer at 1 G field modulation and 100 G scan range with 20 mW microwave power. Transmission electron microscopy (TEM) images were obtained from FEI Tecnai G2 F20 with an accelerating voltage of 200 kV. Scanning electron microscopy (SEM) images were taken by Quattro S (Thermo Scientific) and the samples were dried and coated with Au before measurements. Dynamic light scattering (DLS) profiles were recorded on Malvern Nano ZSE. The cellular fluorescence images were taken in a confocal laser scanning microscope (ZEISS LSM900). Mouse NIR bioimaging data from PerkinElmer's IVIS Spectrum. The photothermal images and temperature changes were recorded on an IR thermal camera (FLIR-E53).

Theoretical calculations

All electronic structure calculations were conducted using Gaussian 16 program [1]. The geometry optimizations were performed at the B3LYP-D3/6-31G(d) level [2]. There were no imaginary vibrational frequencies indicating that the optimized geometries were at local energy minima. On the basis of def2-TZVP, the electron excitation energy was calculated in the assumed nonequilibrium solvation. To be consistent with the experiment, the THF solvent was considered and the SMD solvation effects [3] model was chosen. The natural transition orbitals (NTO) [4] and the distance between centroid of hole and electron (D) [5] were performed by Multiwfn [6] and visualized by VMD [7].

Synthesis of organic ligand TPA-BTZ



Scheme S1. Synthetic route of the TPA-BTZ.

TPA-BTZ was synthesized via Suzuki coupling reaction. In practice, 4,8-dibromo-6-(2-ethylhexyl)-[1,2,5]thiadiazole [3,4-F]benzotriazole (0.13 mmol, 100 mg) and 4-(Diphenylamino)phenylboronic acid (0.69 mmol, 121 mg) were added in toluene/water mixed solution (30 mL) containing 90 mg dry K_2CO_3 . Subsequently, Tetrakis(triphenylphosphine)palladium (6.5×10^{-3} mmol, 7.5 mg) as the catalyst was added at room temperature under N_2 atmosphere. Subsequently, the mixed solution was heated to 85 °C followed by stirring for 3 days. Then the mixture solution was cooled to room temperature followed by solvent evaporation under reduced pressure. The desired blue compound was obtained by purification with silica gel column (DCM/Hexane = 1:1). Yield: 75%. 1H NMR (600 MHz, Chloroform-d) δ 8.40-8.38 (d, $J = 12$ Hz, 4H), 7.32 – 7.30 (t, $J = 6$ Hz, 8H), 7.27-7.23 (t, $J = 6$ Hz, 12H), 7.10 – 7.07 (t, $J = 6$ Hz, 4H), 4.81-4.79 (d, $J = 12$ Hz, 2H), 0.98-0.96 (t, $J = 6$ Hz, 3H), 0.86-0.84 (t, $J = 6$ Hz, 3H). ESI-MS (m/z): calcd. for $C_{50}H_{45}N_7S$ $[M]^+$, 776.3473; found, 775.3457.

The Lippert-Mataga equation

$$\Delta\nu = \nu_A - \nu_F = \frac{2\Delta\mu^2}{hca^3} \Delta f + const \quad (1)$$

$$\Delta f = \frac{\epsilon - 1}{2\epsilon + 1} - \frac{n^2 - 1}{2n^2 + 1} \quad (2)$$

$$\Delta\mu = \mu_e - \mu_g \quad (3)$$

$$a_0 = \left(\frac{3M}{4N\pi d} \right)^{\frac{1}{3}} \quad (4)$$

Where $\Delta\nu$ is the Stokes shift in cm^{-1} between the absorption and emission wavelength. $\Delta\mu$ is the difference of dipole moments between the ground states and excited states. The orientation polarizability Δf of the solvents is derived from the relative permittivity ε and refractive index n of the solvents. The Onsager cavity radius a_0 is expressed by molecular weight M , the Avogadro number N , and density d ($1.0 = \text{g/cm}^{-3}$). Based on equation (4), the a_0 of TPA-BTZ is calculated to be 6.750 \AA .

Preparation of TPA-BTZ@PEG2000

TPA-BTZ@PEG2000 nanoparticles (NPs) were obtained based on the well-documented nanoprecipitation method.[8] Firstly, PEG2000 (5mg) and TPA-BTZ (1 mg) were both dissolved in the common solvent THF. Then 5 mL of deionized water was quickly added followed by ultrasonication for 10 min. Subsequently, the prepared mixed solution was dialysis against a large amount of water for 72 h to remove THF. At last, TPA-BTZ@PEG2000 blue colloid (0.2 mg/mL) was obtained for further characterization.

Photothermal performance of TPA-BTZ@PEG2000 NPs

In general, TPA-BTZ@PEG2000 NPs with different concentrations were exposed to a 634 nm laser. The temperature changes and the corresponding IR thermal images of the sample tubes were recorded by FLIR E50. Photostability was measured by the following procedure: The aqueous solution of TPA-BTZ@PEG2000 NPs (100 μM) was under repeated laser irradiation on-off cycles for 5 times (635 nm, 0.3 W cm^{-2}).

Evaluation of Photothermal conversion efficiency (PCE) of TPA-BTZ@PEG2000 NPs

PCE (η) of TPA-BTZ@PEG2000 NPs (258 μM) was evaluated by employing a 635 nm laser (0.4 W cm^{-2}) as the light source. The temperature of the NPs solutions in water (200 μL) was recorded by real-time measurement with an IR thermal camera (Flir E-

53). When the temperature reached equilibrium, the sample was not irradiated by laser followed by cooling to room temperature without disturbing, and the temperature was recorded at each 15 s during this process.

The PCE (η) was calculated according to the reported method [9]:

$$\eta = \frac{hS(T_{max} - T_{e.t.}) - Q_{dis}}{I(1 - 10^{-A_{634}})} \quad (3)$$

Where h was the heat transfer coefficient, S represented the surface area of the container, T_{max} referred to the maximum equilibrium temperature while $T_{e.t.}$ was the environmental temperature, Q_{dis} presented the heat dissipation caused by the quartz sample cell and solvent, I was the laser power (0.4 W cm^{-2}), and A_{634} was the absorbance of the samples at 634 nm.

In this formula, hS can be obtained from the following formula:

$$\tau = \frac{mC_{H2O}}{hS} \quad (4)$$

Where m and C_{H2O} were a constant and denoted as the mass and heat capacity of the solution ($m = 0.2 \text{ g}$, $C_{H2O} = 4.2 \text{ J} \cdot \text{g}^{-1} \cdot \text{°C}^{-1}$), respectively. τ was the time constant of the sample system calculated by the following equation:

$$t = -\tau \ln \theta, \quad \theta = \frac{T - T_{e.t.}}{T_{max} - T_{e.t.}} \quad (5)$$

Where t was time, and T was the sample temperature.

Cell culture

The tumor cell model used *in vitro* study was 4T1 cells. The specific cell culture approach was shown below:

4T1 cells were cultured in a similar procedure. 4T1 cells were incubated in RPMI 1640 Medium containing 10% fetal bovine (FBS) serum and 1% penicillin-streptomycin (penicillin 10000 U/mL, streptomycin 10 mg/mL) at 37 °C with 5% carbon dioxide.

Cell uptake of the TPA-BTZ@PEG2000 NPs

4T1 cells were incubated with TPA-BTZ@PEG2000 NPs (20 $\mu\text{g}/\text{mL}$). Then 4T1 cells treated with TPA-BTZ@PEG2000 NPs were cultured in different time intervals (2 h, 6 h, 12 h, and 24 h) at 37 °C. After each interval, 4T1 cells were stained with 250 μL DAPI (1 \times) for 10 minutes followed by washing with PBS solution three times. Before the images were taken, the cells were fixed with 4 % Paraformaldehyde for 15 minutes and washed 3 times with FBS. The cell images were taken by a confocal laser scanning microscope (ZEISS LSM900).

Intracellular $^1\text{O}_2$ evaluation

The intracellular $^1\text{O}_2$ efficiency was evaluated with ROS probe SOSG or DCFH-DA. Firstly, the 4T1 cells were first treated with TPA-BTZ@PEG2000 NPs (30 μM) and cultured at 37 °C. After incubation for 24 h, 4T1 cells were fixed with 4 % Paraformaldehyde for 15 minutes followed by washing 3 times with PBS. Subsequently, 4T1 the cells were stained with 250 μL SOSG (5 μM), DHE (10 μM), or DCFH-DA (15 μM) for 15 min and then washed 3 times with PBS buffer solution. The cell fluorescence images before or after light irradiation (635 nm, 0.4 $\text{W}\cdot\text{cm}^{-2}$, 2 min) were obtained by a confocal laser scanning microscope (ZEISS LSM880).

Cell viability assay

The phototoxicity of TPA-BTZ@PEG2000 NPs to 4T1 cells was evaluated by standard methylthiazole tetrazole (MTT) assay. In general, the cells were firstly incubated on 96-well culture plates at a density of 6×10^3 cells per well in the above culture medium for 24 hours. Subsequently, the cells were treated with TPA-BTZ@PEG2000 NPs with various concentrations ranging from 5 to 40 μM (based on TPA-BTZ) and incubated for another 12 hours. After that, the cells were washed three times with PBS and replaced with a fresh medium. Then, the 4T1 cells were exposed to laser irradiation (635 nm, 400 $\text{mW}\cdot\text{cm}^{-2}$, 5 min) before further incubation for 12 h. The dark group was performed with a similar procedure without light irradiation. Then 100 μL MTT solution (0.5 mg/mL) was added into each well and the cells were cultured for another

4 h. At last, DMSO was used to dissolve the formed formazan crystals and the cell viability was evaluated by the enzyme plate analyzer.

PDT or PTT solely experiment was evaluated with a similar procedure. In solely PTT test, the cells were cultured with N-acetylcysteine (NAC, a ROS scavenger) to react with ROS generated by TPA-BTZ@PEG2000 NPs upon laser irradiation. In solely PDT, the culture plates were put on ice to keep the cells cool when laser irradiated the medium.

***In vitro* PDT cytotoxicity assay in a hypoxic atmosphere**

The 4T1 cells were first cultured in 96 well plates for 16 h under a normoxic (21% O₂) atmosphere followed by incubation for another 8 h under a hypoxic atmosphere (1% O₂). After 24 h, TPA-BTZ@PEG2000 NPs with various concentrations were added to the plate. And then the cells were incubated for another 24 under a hypoxic atmosphere. The 4T1 cells were irradiated by laser (635 nm, 0.4 W·cm⁻²) for 5 min on an ice bath to keep the well cool before incubation for another 24 h under hypoxia. Then 100 μL MTT solution (0.5 mg/mL) was added into each well and the cells were cultured for another 4 h under a normoxic atmosphere. At last, DMSO was used to dissolve the formed formazan crystals and the cell viability was evaluated by the enzyme plate analyzer.

Fluorescence imaging in 4T1 tumor model.

All animal experiments are carried out based on the protocols approved by the Ethical Committee of Shandong University under production license number SCXK 2019-0001 and use license number SYXK 2019-0005. BALB/c female mice aged 8 weeks were purchased from Jinan PengYue Experimental Animal Breeding Co., Ltd, China. 4T1 cells were firstly collected and dispersed in PBS to prepare 4T1 cell suspension at a density of 5×10⁷ mL⁻¹. Then 100 μL of the above cell fluid was injected into the subcutaneous area of each mouse. The tumor-bearing mice were orthotopically injected with an aqueous dispersion of TPA-BTZ@PEG2000 NPs (0.26 mM), and fluorescence imaging at different times (12 h, 24 h, 36 h, 6 days, 12 days, 14 days post-injection) was recorded using an IVIS Spectrum system (PerkinElmer) with a 635 nm pulsed

diode laser and near-infrared fluorescence emission (700 - 800 nm). The final processing used the built-in software of the imaging system (parameter settings: min = $4.00e^8$, Max = $1.00e^9$).

***In vivo* antitumor performance in the 4T1 tumor model**

4T1 cells were inoculated into the subcutaneous area of the left armpit (tumor density of 5×10^7 mL⁻¹ per mouse). Four days later, Balb/c mice bearing 4T1 tumors were randomly divided into 3 groups: (1) TPA-BTZ@PEG2000-light, (2) TPA-BTZ@PEG2000-dark group, and (3) saline-light. After the tumor volume reached *ca.* 90 mm³. TPA-BTZ@PEG2000 or saline (100 μ L) was orthotopically injected into mice. After 24 hours, the first laser irradiation (635 nm, 0.4 W cm⁻²) was conducted and the day was considered day 0 of 4T1 tumor treatment. Then tumor sizes were measured three times every 2 days meanwhile the body weights were recorded. The related photographs of mice were recorded as well. Note: Tumor volume = (length \times width²)/2.

***Ex vivo* histology examination**

4T1 tumor-bearing mice were sacrificed after treatment. Major organs (heart, liver, spleen, lung, and kidney) and tumors of the treated mice were collected for hematoxylin and eosin (H&E) staining. These tissues were embedded in paraffin cassettes and related fluorescence images were recorded by a fluorescent microscope.

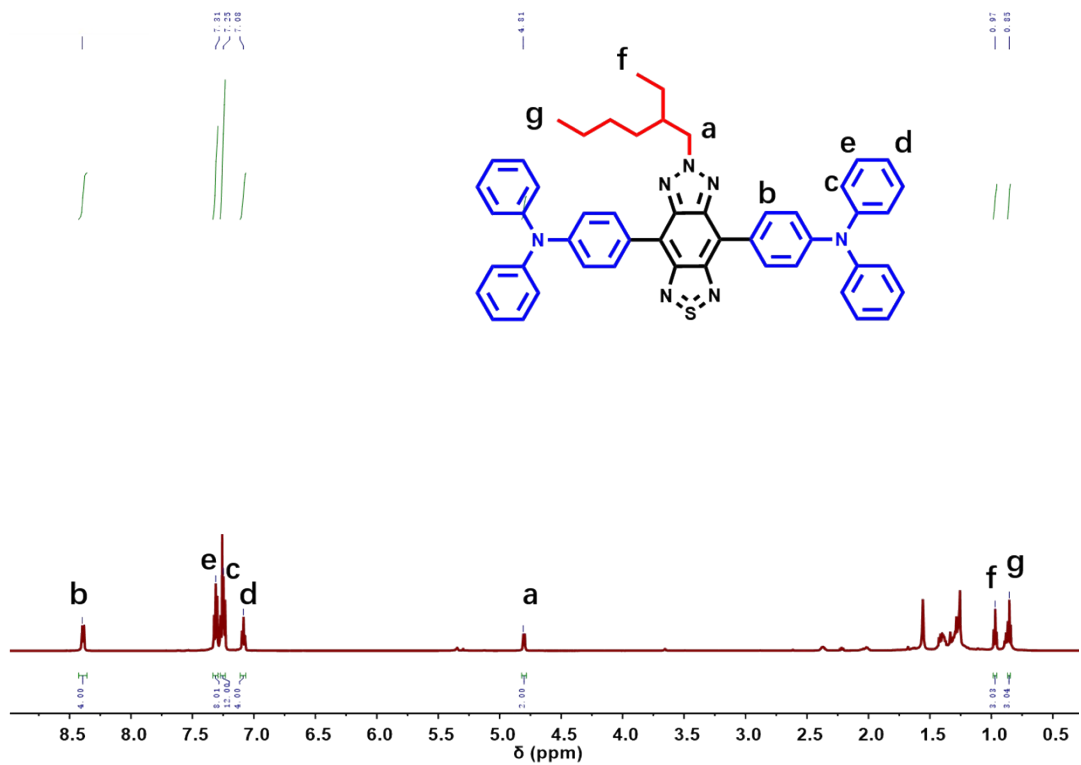


Figure S1. ¹H NMR spectrum of TPA-BTZ in CDCl₃ at 298 K.

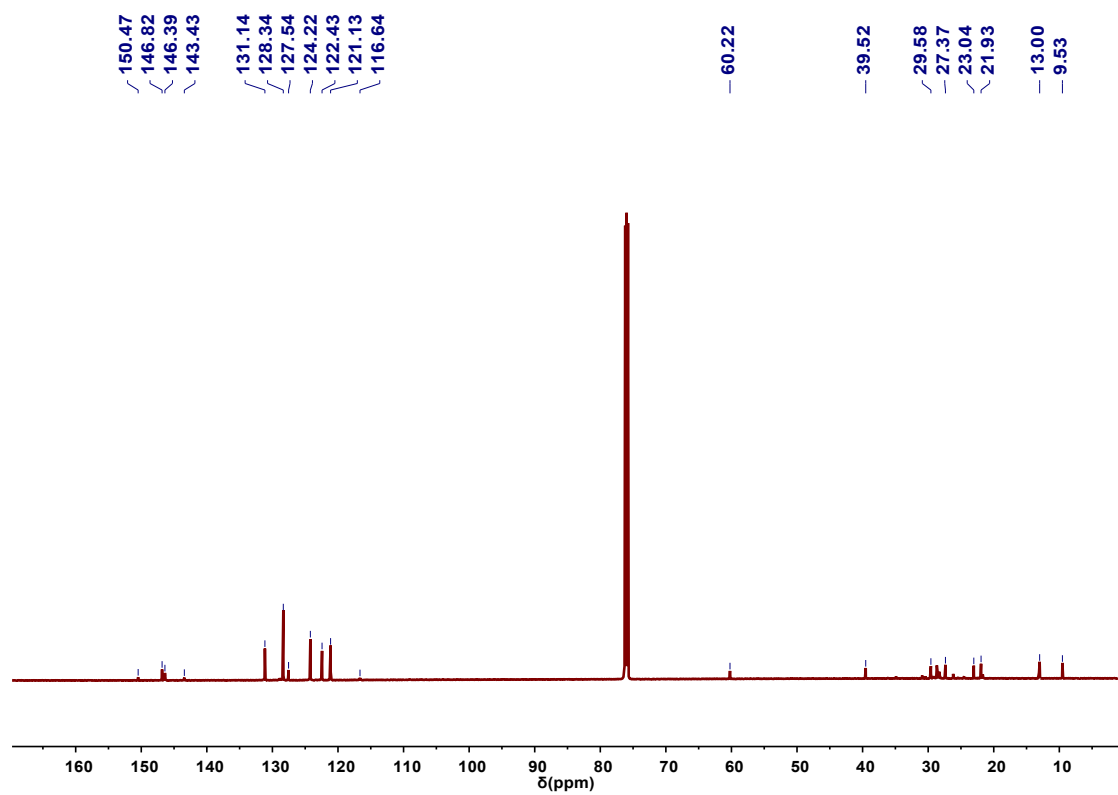


Figure S2. ¹³C NMR spectrum of TPA-BTZ in CDCl₃ at 298 K.

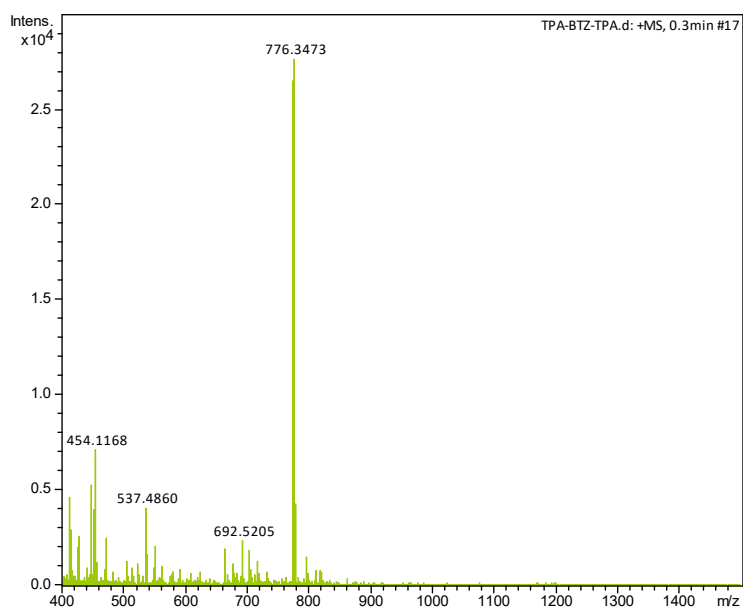


Figure S3. ESI-MS of TPA-BTZ.

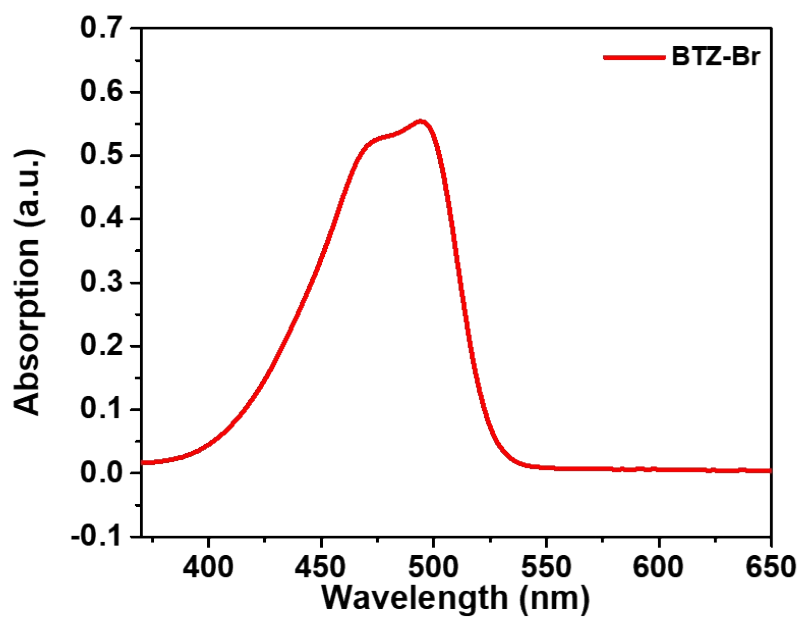


Figure S4. UV-Vis absorption spectrum of BTZ-Br in tetrahydrofuran (THF).

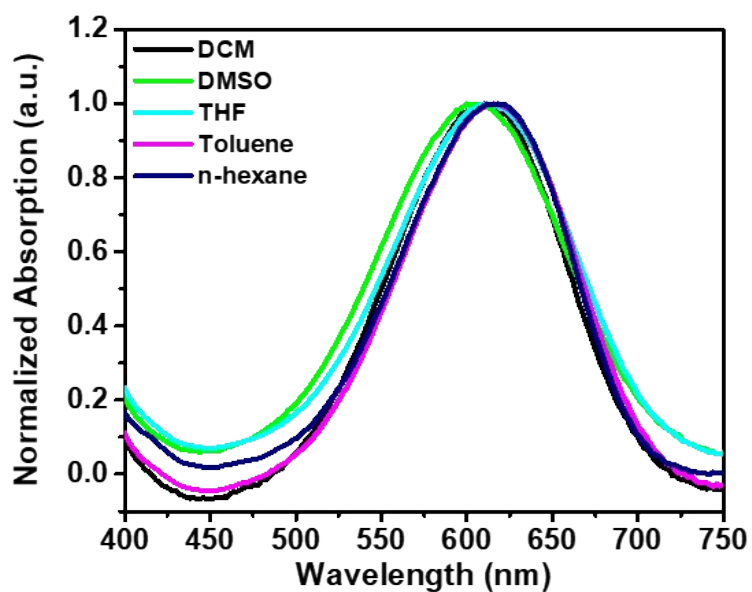


Figure S5. UV-Vis absorption spectra of TPA-BTZ in different solvents. (Toluene, n-hexane, THF, DCM, DMSO).

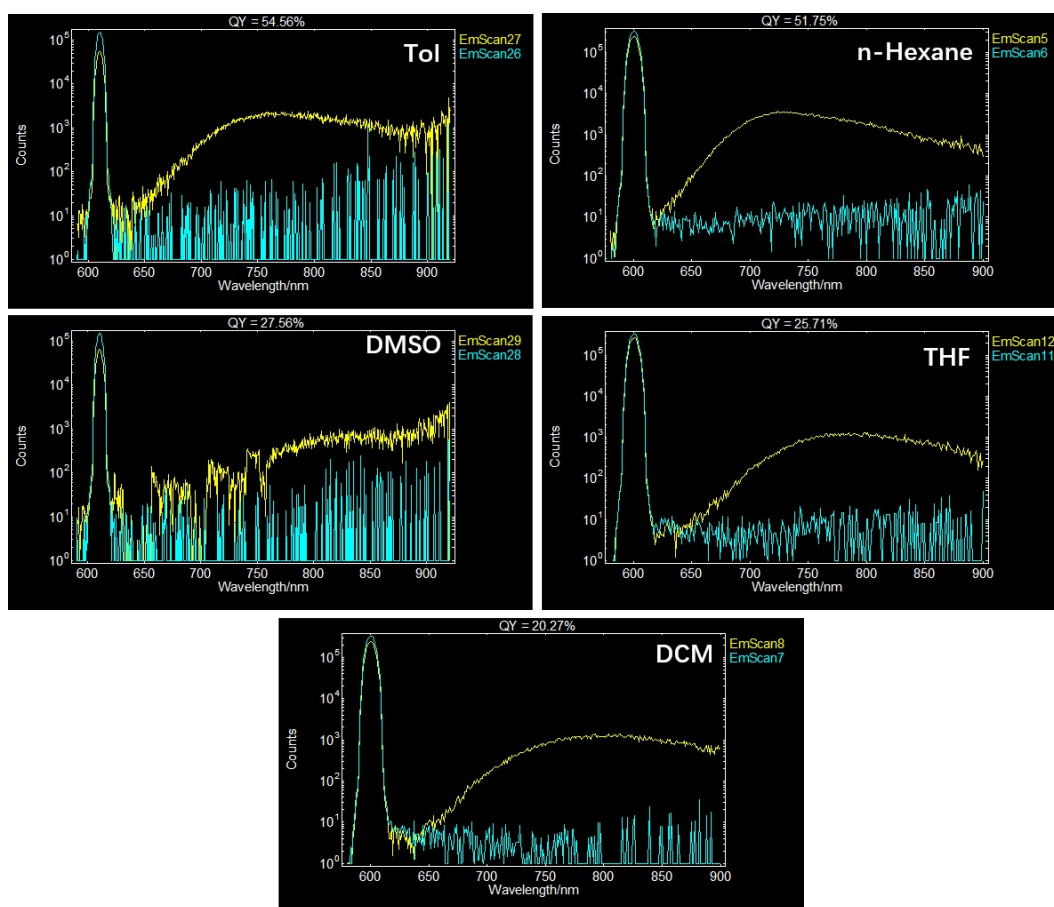


Figure S6. The absolute fluorescence quantum yields (QYs) of TPA-BTZ in different solvents.

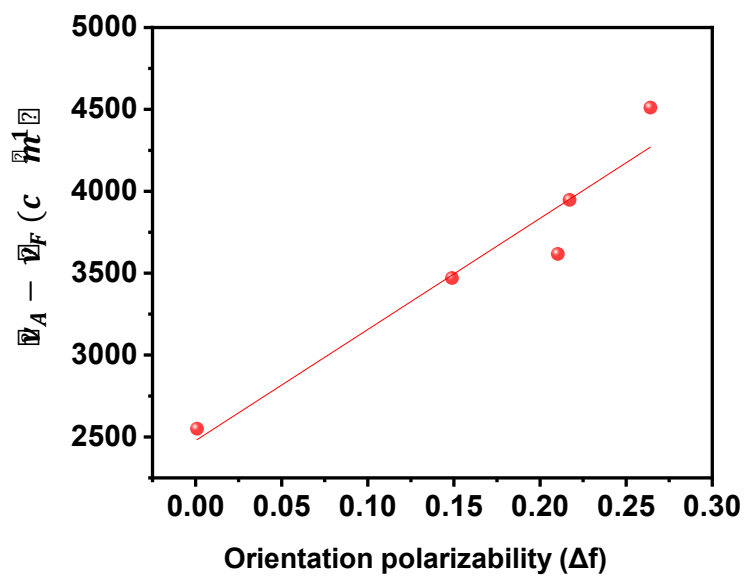


Figure S7. The Lippert-Mataga plot for TPA-BTZ in different solvents. The slope of the fitting line is 6786 cm⁻¹ (R² = 0.93).

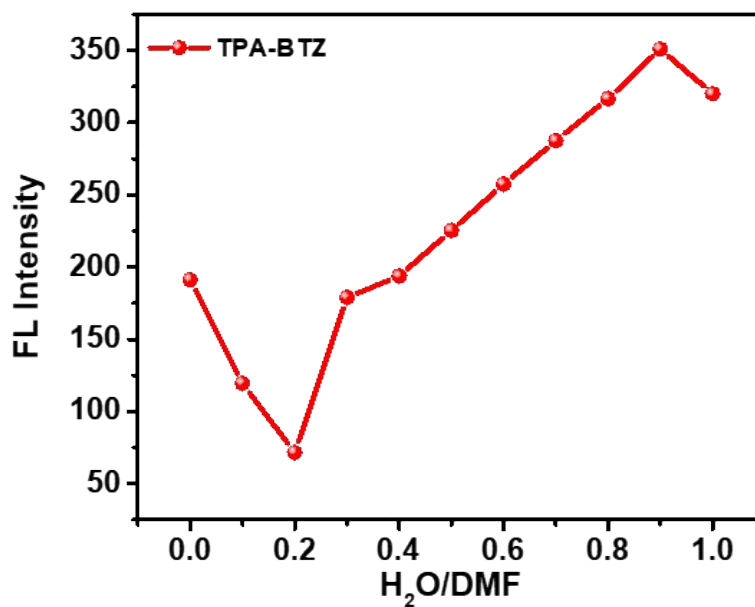


Figure S8. The FL intensity of the compound TPA-BTZ as a function of water content in the mixed H₂O/DMF system.

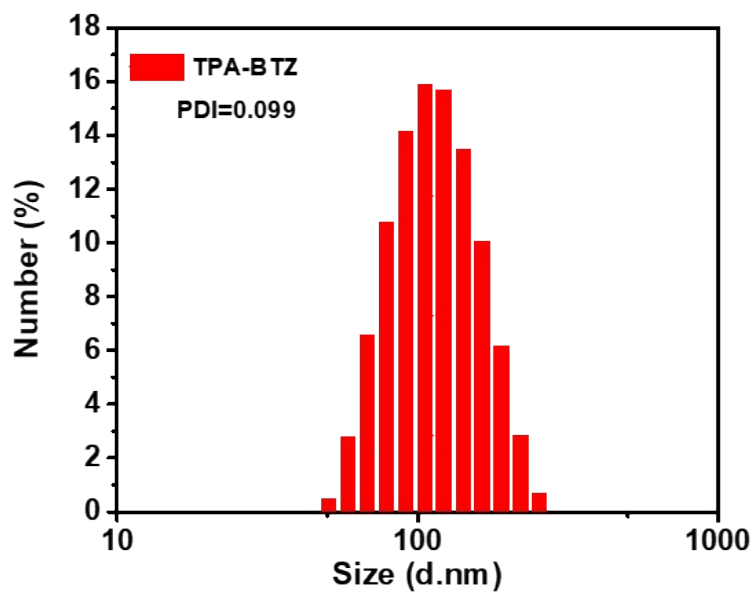


Figure S9. The hydrodynamic diameter of the TPA-BTZ aggregates in the mixed solvent DMF/H₂O (90% water content).

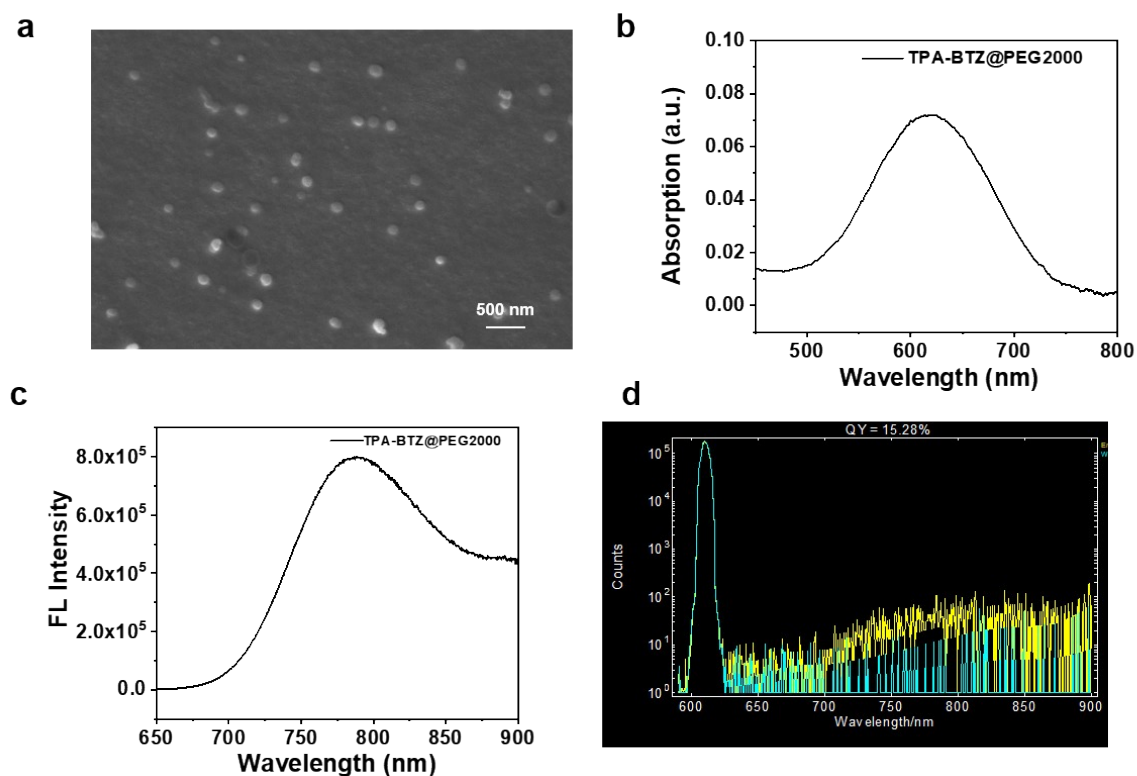


Figure S10. The SEM image (a), UV-vis absorption (b), FL emission spectra (c), and QYs (d) of TPA-BTZ@PEG2000 NPs in water.

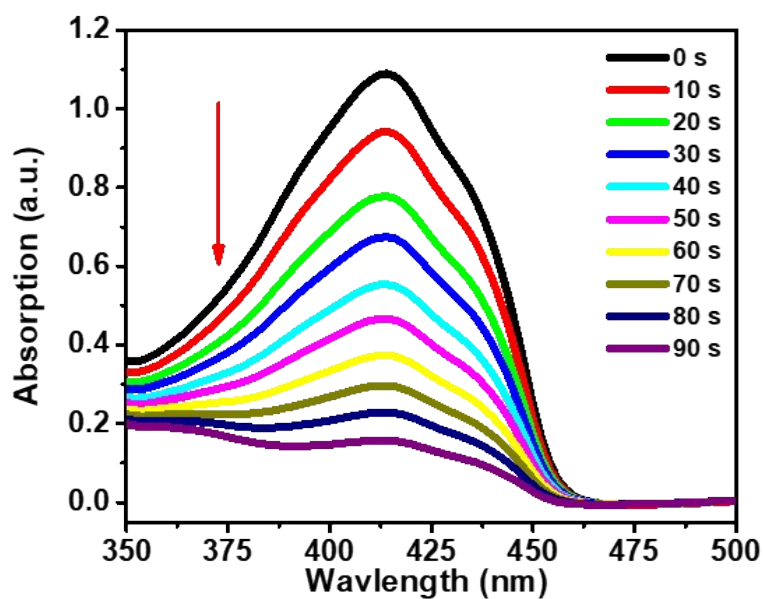


Figure S11. Absorption changes of DPBF treated with TPA-BTZ@PEG2000 NPs (10 μ M) upon laser irradiation at different times.

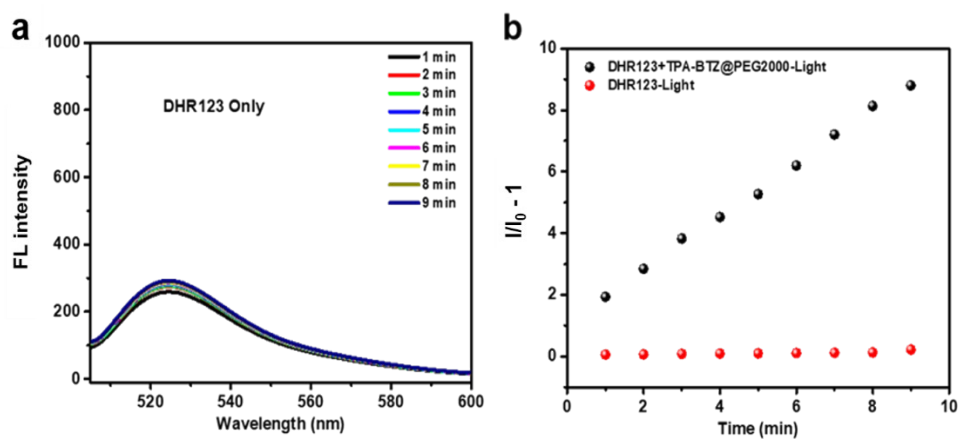


Figure S12. a) FL emission spectra of DHR123 (a control group) under laser irradiation for different times. b) Relative fluorescence emission intensity changes of DHR123 in the presence or absence of TPA-BTZ@PEG2000 NPs upon illumination for different times. DHR (10 μ M)

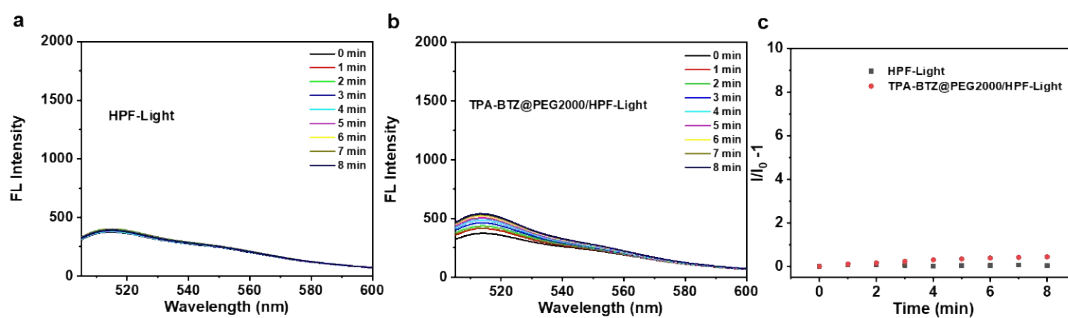


Figure S13. FL emission spectra of HPF without (a) /with (b) of TPA-BTZ@PEG2000 NPs under laser irradiation for different times. c) Relative fluorescence emission intensity changes of HPF in the presence or absence of TPA-BTZ@PEG2000 NPs upon illumination for different times. HPF (10 μ M)

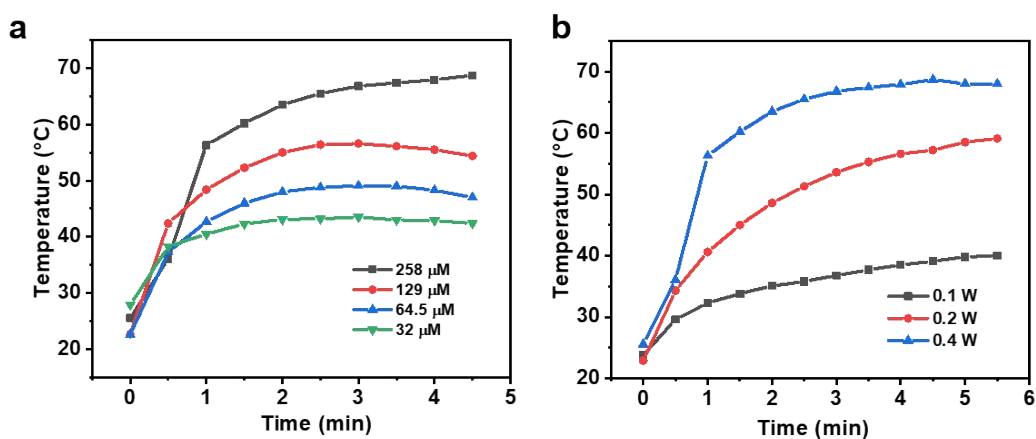


Figure S14. a) Concentration-dependent temperature variation of TPA-BTZ@PEG2000 NPs under laser irradiation (635 nm, $0.4 \text{ W} \cdot \text{cm}^{-2}$). b) Laser power-dependent temperature variation of TPA-BTZ@PEG2000 NPs (0.26 mM) under laser irradiation (635 nm).

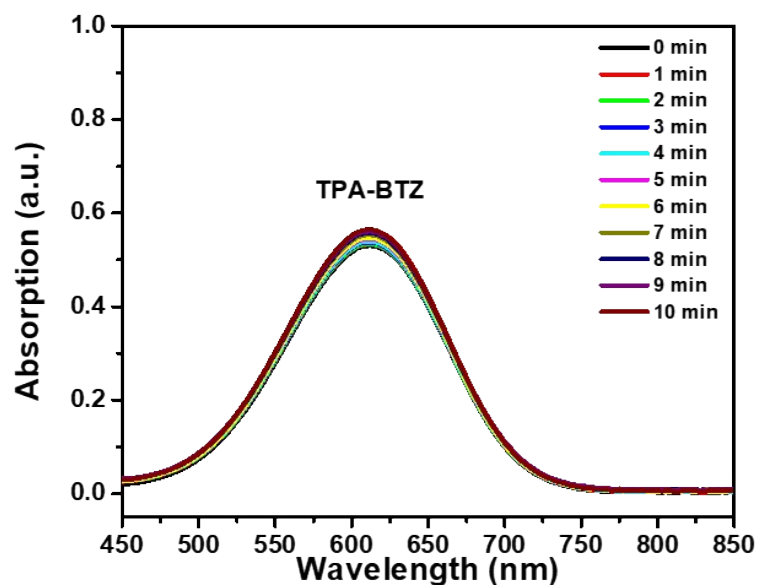


Figure S15. Absorption spectra of TPA-BTZ upon laser irradiation (635 nm, 0.4 W·cm²) for different times.

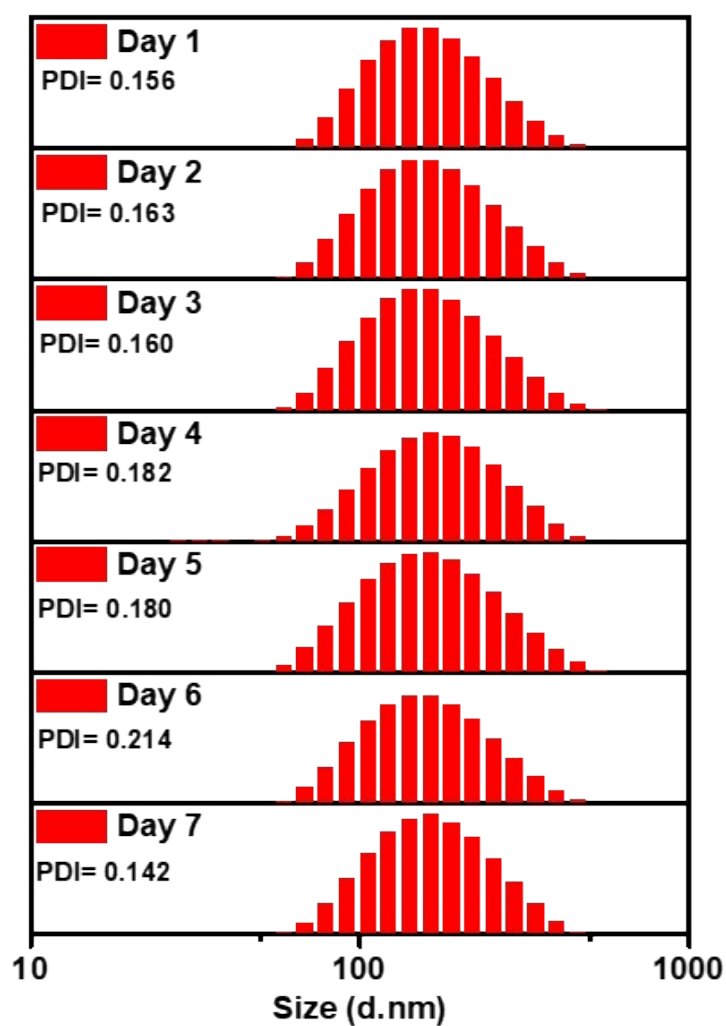


Figure S16. Time-dependent DLS profiles of TPA-BTZ@PEG2000 NPs in water.

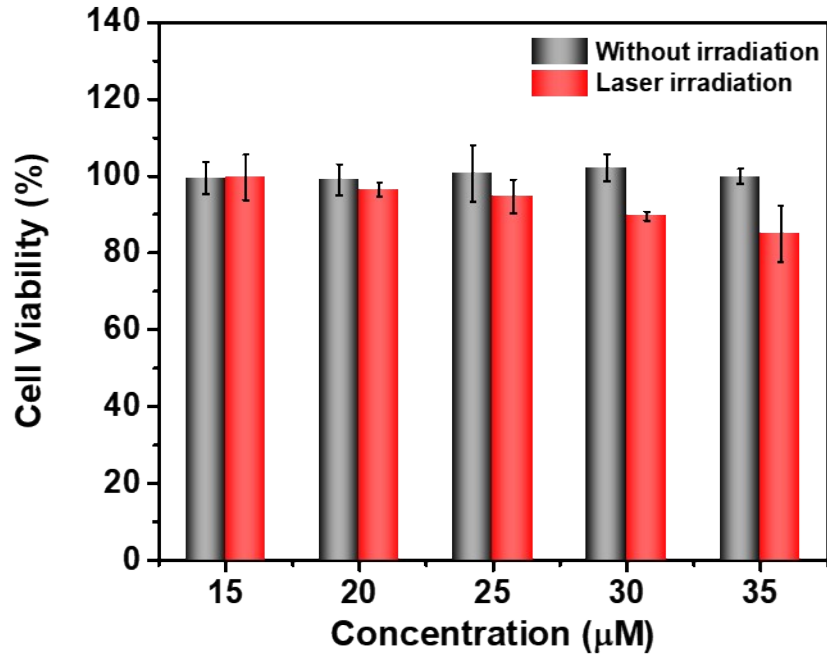


Figure S17. Cell viability of 4T1 cells cultured with various concentrations of TPA-BTZ@PEG2000 NPs after laser irradiation (635 nm, $0.4 \text{ W} \cdot \text{cm}^{-2}$) on ice for 5 min under hypoxia.

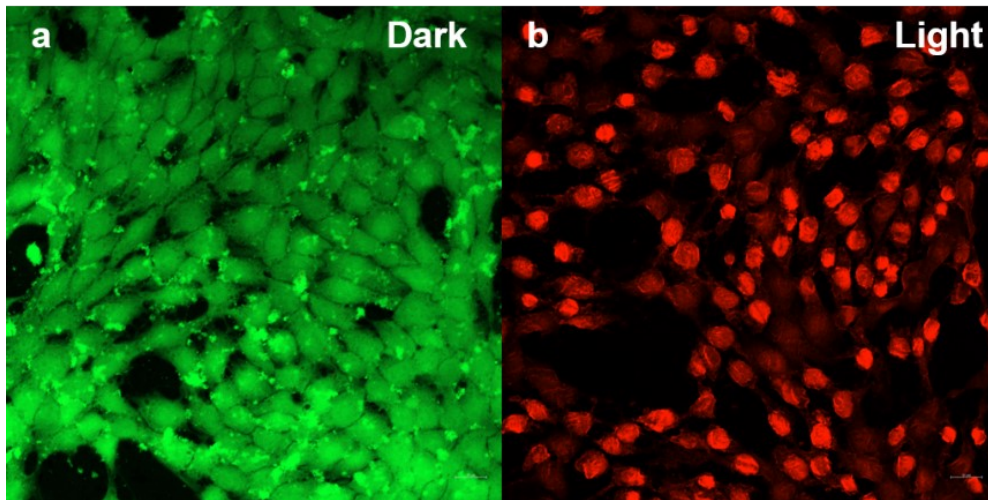


Figure S18. Fluorescence images of calcein (AM, green) and propidium iodide (PI, red) contained 4T1 cells after treatments with/without laser irradiation (635 nm, $0.4 \text{ W} \cdot \text{cm}^{-2}$). The green and red colors represent live cells and dead cells, respectively.

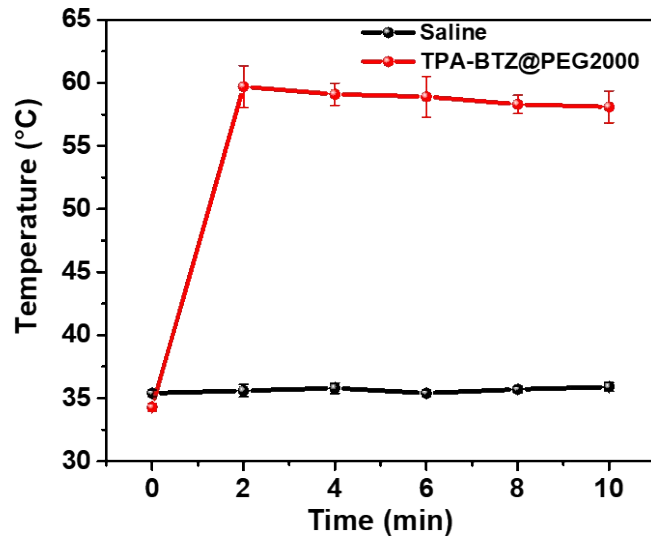


Figure S19. Temperature as a function of time in 4T1 tumors of mice treated with saline / TPA-BTZ@PEG2000 NPs under laser irradiation (635 nm, $0.4 \text{ W} \cdot \text{cm}^{-2}$).

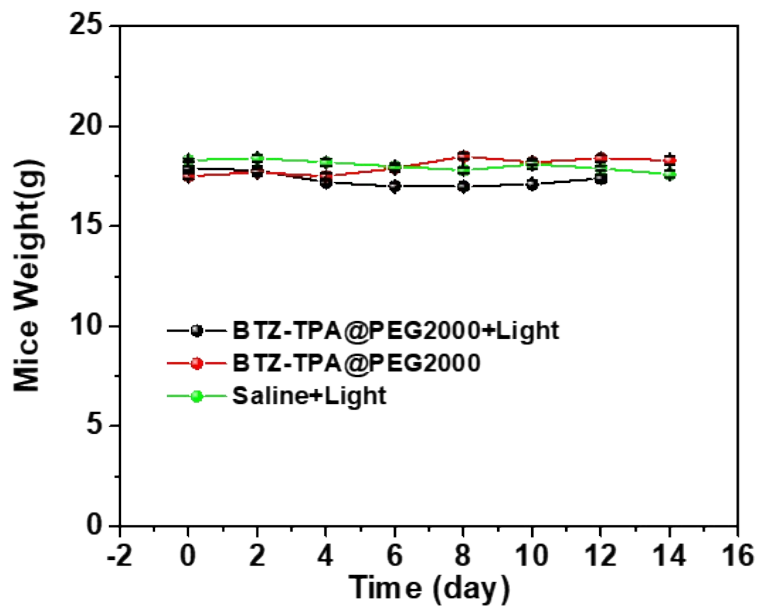


Figure S20. Body weights of the mice in different groups as a function of time.

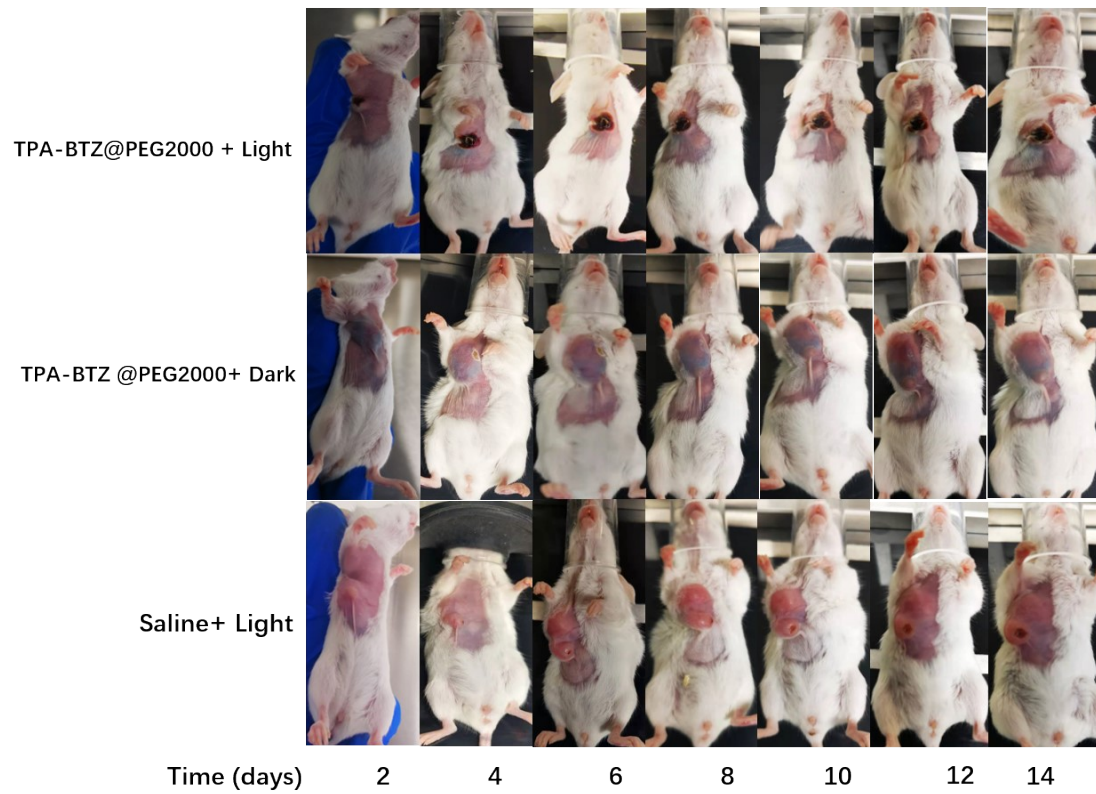


Figure S21. Photographs of the tumors in the 4T1 tumor-bearing mice with different treatments.

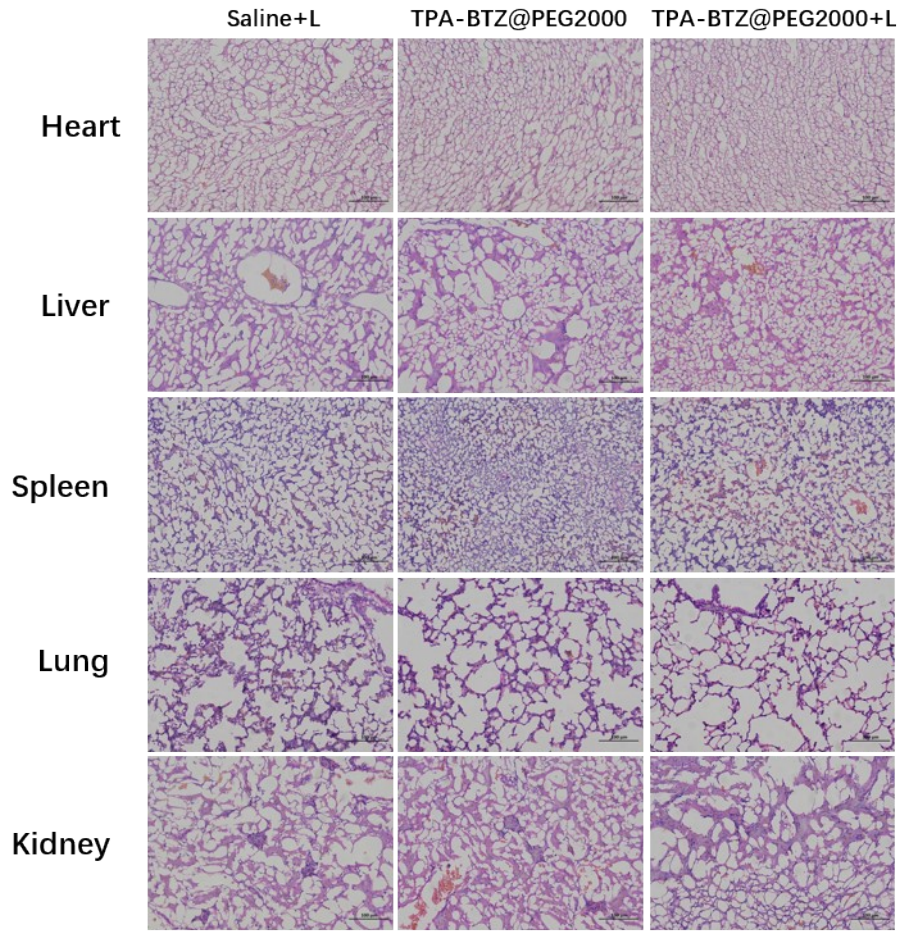


Figure S22. Histochemical analysis of heart, liver, spleen, lung, and kidney.

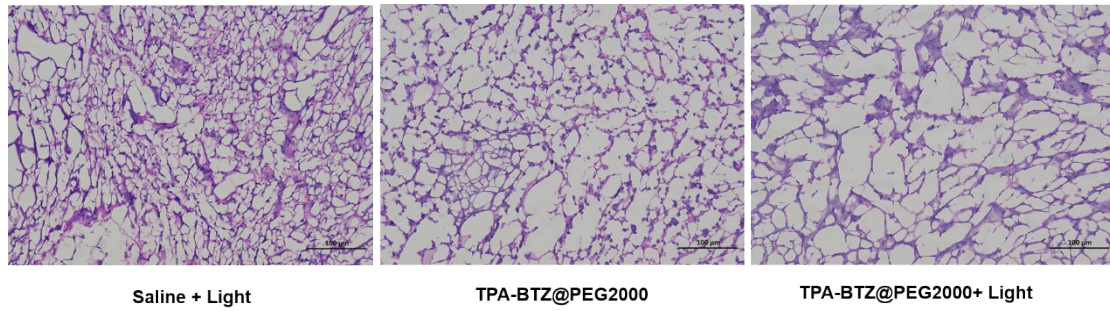


Figure S23. Hematoxylin and eosin (H&E) staining analysis of tumor tissues after different treatments.

Table S1. Absorption, emission wavelengths, and QYs of TPA-BTZ in different organic solvents at 298 K.

Solution	Absorption (nm)	Emission (nm)	Quantum Yields (QYs)
Toluene	616	766	54.56%
n-hexane	614	726	51.75%
DMSO	600	840	27.26%
THF	612	786	25.71%
DCM	610	796	20.27%

Table S2. The relative permittivity ϵ , refractive index n , and the orientation polarizability Δf of different solvents, and Stoke shifts (cm^{-1}) of TPA-BTZ in various solvents.

Solvents	ϵ	n	Δf	$\lambda_{abs}(nm)$	$\lambda_{em}(nm)$	$\Delta\nu(\text{cm}^{-1})$
n-hexane	1.889	1.372	0.001	614	728	2550
Chloroform	4.81	1.444	0.149	620	790	3471
THF	7.58	1.405	0.210	612	786	3617
DCM	8.93	1.4242	0.217	608	800	3947
DMSO	48.9	1.4783	0.264	606	834	4511

References

- [1] Gaussian 16, Revision B.01, M. J. Frisch, G. W. Trucks, H. B. Schlegel, G. E. Scuseria, M. A. Robb, J. R. Cheeseman, G. Scalmani, V. Barone, G. A. Petersson, H. Nakatsuji, X. Li, M. Caricato, A. V. Marenich, J. Bloino, B. G. Janesko, R. Gomperts, B. Mennucci, H. P. Hratchian, J. V. Ortiz, A. F. Izmaylov, J. L. Sonnenberg, D. Williams-Young, F. Ding, F. Lipparini, F. Egidi, J. Goings, B. Peng, A. Petrone, T. Henderson, D. Ranasinghe, V. G. Zakrzewski, J. Gao, N. Rega, G. Zheng, W. Liang, M. Hada, M. Ehara, K. Toyota, R. Fukuda, J. Hasegawa, M. Ishida, T. Nakajima, Y. Honda, O. Kitao, H. Nakai, T. Vreven, K. Throssell, J. A. Montgomery, Jr., J. E. Peralta, F. Ogliaro, M. J. Bearpark, J. J. Heyd, E. N. Brothers, K. N. Kudin, V. N. Staroverov, T. A. Keith, R. Kobayashi, J. Normand, K. Raghavachari, A. P. Rendell, J. C. Burant, S. S. Iyengar, J. Tomasi, M. Cossi, J. M. Millam, M. Klene, C. Adamo, R. Cammi, J. W. Ochterski, R. L. Martin, K. Morokuma, O. Farkas, J. B. Foresman, and D. J. Fox, Gaussian, Inc., Wallingford CT, 2016.
- [2] Phys. Rev. A, 38, 3098 (1988); Phys. Rev. B, 37, 785 (1988); JCC,32,1456(2011)
- [3] Marenich, A. V.; Cramer, C. J.; Truhlar, D. G. Universal Solvation Model Based on Solute Electron Density and on a Continuum Model of the Solvent Defined by the Bulk Dielectric Constant and Atomic Surface Tensions. *J. Phys. Chem. B* 2009, 113, 6378–6396.
- [4] Martin, R. L., Natural transition orbitals. *J. Chem. Phys.* 2003, 118 (11), 4775-4777.
- [5] Carbon, 165, 461-467 (2020) DOI: 10.1016/j.carbon.2020.05.023
- [6] Lu T , Chen F . Multiwfn: A multifunctional wavefunction analyzer[J]. *Journal of Computational Chemistry*, 2012, 33(5).
- [7] Humphrey W , Dalke A , Schulten K . VMD: Visual molecular dynamics[J]. *j mol graph*, 1996, 14(1):33-38.
- [8] Nguyen, V.-N.; Yim, Y.; Kim, S.; Ryu, B.; Swamy, K. M. K.; Kim, G.; Kwon, N.; Kim, C.-Y.; Park, S.; Yoon, J., Molecular Design of Highly Efficient Heavy-Atom-Free Triplet BODIPY Derivatives for Photodynamic Therapy and Bioimaging. *Angew. Chem., Int. Ed.* 2020, 59 (23), 8957-8962.
- [9] E. Feng, L. Jiao, S. Tang, M. Chen, S. Lv, D. Liu, J. Song, D. Zheng, X. Peng, F. Song, *Chemical Engineering Journal* 2022, 432, 134355.